5th International Conference on Experimental Fluid Mechanics ICEFM 2018 Munich
Munich, Germany, July 2-4, 2018

A Non-Linear Transport Model for Flow In Tight Porous Media

Iftikhar Ali and Nadeem A. Malik*

Department of Mathematics & Statistics, King Fahd University of Petroleum and Minerals, P.O. Box 5046, Dhahran 31261, Saudi Arabia.

*Corresponding: nadeem_malik@cantab.net

Abstract

A nonlinear transport model with pressure dependent parameters for gas flow in tight porous media [I. Ali and N. A. Malik. Transport In Porous Media Vol. 123 No. 2, (2018)] is used to to determine shale rock properties, such as the porosity and the permeability, and to carry out forward simulations from the transient model. The results show improvment on previous pressure indenpendent transport models.

1 Introduction

Transport models can predict future gas recovery, and they can also be used for determining rock properties, so it is important to develop realistic transport models. However, at present, little is known about gas transport processes through tight rocks. Darcy's law fails for tight porous media because the pore size is nanoscale and the pore network produces several flow regimes, such as slip flow, transitional flow, surface diffusion, and Knudsen flow, and adsorption and desorption of the gas from the rock material also plays a key role. The system is also pressure dependent. Shales have very small pore size compared to conventional rock formations, typically in the range of 50-200 nm Wang et al (2013); Nia et al (2013). Shales also have low porosity, typically in the range 4-15 %, and very low permeability in the range 10-2000 nD, Darishchev et al (2013).

Here, we use the nonlinear transport model developed by Ali and Malik (2018) to determine shale rock properties, such as the porosity and the permeability, and to carry out forward simulations from the transient model.

2 A transport model for flow in tight porous media

Different flow regimes are classified through the Knudsen number, Ziarani and Aguilera (2012), which is defined as the ratio of the molecular mean free path λ to the hydraulic radius R_h, of the flow channels, $K_n = \frac{\lambda}{R_h}$. The Mean Free Path ($\lambda$) is the average distance traveled by a gas molecule between collisions with other molecules. There exists several models for the mean free path, such as given by Loeb (2004), $\lambda = \frac{\mu}{p}\sqrt{\frac{\pi R_g T}{2M_g}}$, where T is the absolute temperature (K), R_g is the universal gas constant and M_g is the molecular weight of gas. The hydraulic radius R_h is the mean radius of a system of pores Carman and Carman (1956); Civan (2010) and is given by $R_h = 2\sqrt{2\tau_h}\sqrt{\frac{K}{\phi}}$, where ϕ is the porosity, and τ_h is the tortuosity which is the ratio of apparent length of the effective mean hydraulic tube to the physical length of the bulk porous media.

Flow regimes are defined in different ranges of the Knudsen number, illustrated in Fig. 1. Viscous flow occurs when $\lambda << R_h$ and can be described by Darcy's law; Knudsen flow occurs when $\lambda >> R_h$, Darcy's law completely fails in this regime; Slip flow occurs due to accumulation of gas molecules along the pore surface.

Mass conservation, including the loss of mass of gas by adsorption in to the bulk volume of porous medium, is given by,

$$\frac{\partial(\rho\phi)}{\partial t} + \frac{\partial[(1-\phi)q]}{\partial t} = -\nabla\cdot(\rho\mathbf{u}) + Q \tag{1}$$

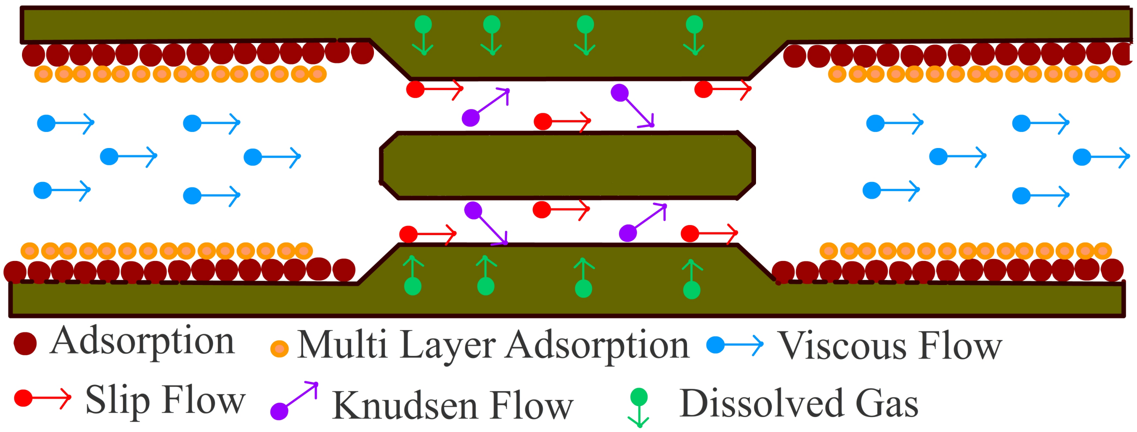

Figure 1: Viscous flow occurs when $\lambda << R_h$ and can be described by Darcy's law; Knudsen flow occurs when $\lambda >> R_h$, Darcy's law completely fails in this regime; Slip flow occurs due to accumulation of gas molecules along the pore surface.

where ρ is the gas density, q is the mass of gas absorbed per solid volume of rock, and Q is some external source. Momentum conservation, through a modified Darcy's law with a non-linear Forchheimer term correction for high flow rates (turbulence), is given by,

$$-(\nabla p - \rho g \nabla H) = \mu \mathbf{K}_a^{-1} \cdot \mathbf{u} + \rho \mathbf{B} |\mathbf{u}| \cdot \mathbf{u} = \mu \mathbf{K}_a^{-1} \left(\mathbf{I} + \frac{\rho}{\mu} \mathbf{B} \mathbf{K}_a |\mathbf{u}| \right) \cdot \mathbf{u} \tag{2}$$

where p is the pressure, $\mathbf{u}$ is the volumetric flux, μ (Pa s) is the dynamic viscosity of the flowing gas, g (m^2/s) is the magnitude of the gravitational acceleration vector, $\mathbf{K}_a$ (m^2) denotes the apparent permeability tensor of the rock, and $\mathbf{B}$ represents the inertial and turbulence effects where the velocity is high, it is considered to be a function of $\mathbf{K}_a$, ϕ, and τ. Furthermore, ϕ, μ, ρ are functions of pressure p.

From these equations, the most general transport equation for the pressure field in a single-phase gas flow in tight porous media in three-dimensions, incorporating the various flow regimes, and including gravity and a source term, is given by Ali and Malik (2018),

$$\begin{aligned} \frac{\partial p}{\partial t} &= \mathbf{D}_a(p) : \nabla \nabla p + {}_3(p) \nabla p \cdot \mathbf{D}_a(p) \cdot \nabla p \\ &- \rho g \mathbf{D}_a : \nabla \nabla H - \rho g \zeta_3(p) \nabla p \cdot \mathbf{D}_a \cdot \nabla H - \nabla(\rho g) \cdot \mathbf{D}_a \cdot \nabla H + \zeta_t(p) Q \end{aligned} \tag{3}$$

H (m) is the depth function, $\mathbf{D}_a$ (m^2/s) is the the apparent diffusivity tensor. $\zeta_3(p)$ and $\zeta_t(p)$ are compressibility coefficients (defined below).

There are many inter-related physical parameters in this model, and to complete the model in equation (3), we need correlations that define these relationships. An other important relation is the correlation between the intrinsic permeability and the apparent permeability which appears in the model, Beskok and Karniadakis (1999), $\mathbf{K}_a = \mathbf{K} f(K_n)$, where $f(K_n)$ is the flow condition function and is given by $f(K_n) = (1 + \sigma K_n)(1 + \frac{4K_n}{1 - bK_n})$, σ is called the rarefaction coefficient correlation. Formulae for σ and other correlations are given in Ali and Malik (2018).

A key feature of the present model is that in order to include as much physical realism in to the model as possible, all model parameters are pressure dependent throughout the simulations – most previous models make the parameters to be constants. Pressure dependency means that compressibility coefficients exist in the model for every pressure dependent parameter to account for the locally changing conditions. A compressibility coefficient, ζ_y for some physical quantity y is defined as the proportional rate of change of a physical quantity with respect to the pressure, $\zeta_y(p) = \frac{1}{y}\frac{\partial y}{\partial p} = \frac{\partial \ln(y)}{\partial p}$. For example, $\zeta_\rho = \partial \ln(\rho)/\partial p$, and similarly for all other pressure dependent parameters, like ζ_K. Through the correlations defined above the compressibility factors are inter-related so that there are only four basic ones, namely ζ_ρ, ζ_f, ζ_K, and ζ_μ, Ali et al (2015); Ali and Malik (2018). In equation (3), ζ_3 and ζ_t is a combination of the four basic compressibility factors.

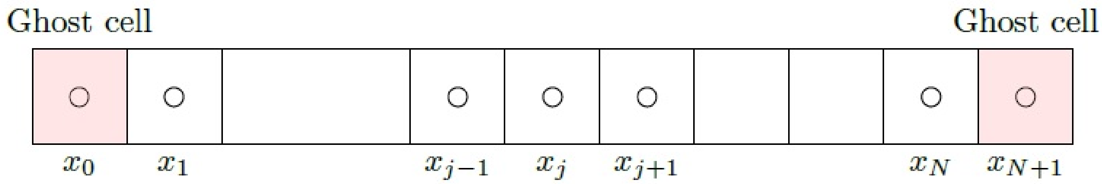

Figure 2: Control volume discretization of the 1-dimensional domain where the points x_j are chosen at the center of the blocks. The left and the right boundary conditions are discretized by taking ghost cells adjacent to the cells containing the point x_1 and the point x_N.

2.1 One-dimensional model

For the simplified one-dimensional system in a horizontal reservoir, without gravity and with no external forcing, equation (3) reduces to,

$$\frac{\partial p}{\partial t} + U_a(p, p_x)\frac{\partial p}{\partial x} = D_a(p)\frac{\partial^2 p}{\partial x^2} \tag{4}$$

where, U_a (m/s), the apparent convective flux (or convective velocity), and $D_a(p)$ (m^2/s) are given by, $U_a = -\zeta_3(p)D_a(p)\frac{\partial p}{\partial x}$ and $D_a(p) = \frac{FK_a}{\mu\zeta_t(p)}$, where F and K_a are now scalar quantities; $F = 1$ if the Forchhiemer non-linear flux correction term is excluded. (See Malkovsky et al (2009), Liang et al (2001), Civan et al (2011) for simplified models.) The further assumption of steady state, $\dfrac{\partial p}{\partial t} = 0$ yields,

$$L_a(p, p_x)\frac{\partial p}{\partial x} = \frac{\partial^2 p}{\partial x^2}, \qquad \text{where} \qquad L_a = -\zeta_3(p)\frac{\partial p}{\partial x}, \tag{5}$$

In model application, $U_a(p)$, $D_a(p)$, $F(p)$, $\zeta_3(p)$, and all the model correlations are assumed known as functions of the pressure, Ali et al (2015); Ali and Malik (2018).

3 Numerical Methods

The nonlinear transport system in equation (1) together with initial and boundary conditions must be solved numerically. Because it is a nonlinear advection-diffusion system, care needs to be taken when high gradients appear in the solution, which is possible when the local Peclet number becomes large. It was found that an implicit finite volume staggered grid arrangement, Figure 2 with the velocity defined on the grid boundaries, with a flux limiter (2nd order van Leer) adequately solved the system. The discretized system produced a tri-diagonal system of nonlinear algebraic equations, $A(p)p = S(p)$, where A is the coefficient matrix, S is the vector of source terms of the right hand side, and p is the pressure vector at all grid points for which we are solving. The matrix equation has to be linearized before inverting, and then iterated to convergence before moving on to the next time step.

4 Determining rock characteristics

4.1 Pressure-pulse decay tests

Rock properties are estimated through an inverse problem whereby model parameters are adjusted to fit a given set of experimental data. Experimental data from pressure-pulse decay test due to Pong et al (1994) are available. In a pressure-pulse decay test a short homogeneous rock sample of length L is initially set to a constant pressure inside the core sample. A pulse of high inlet pressure P_{in} is then sent through the sample from the upstream boundary and the pressure field quickly reaches a steady state distribution across the core length. The pressure is recorded at different stations along the core length.

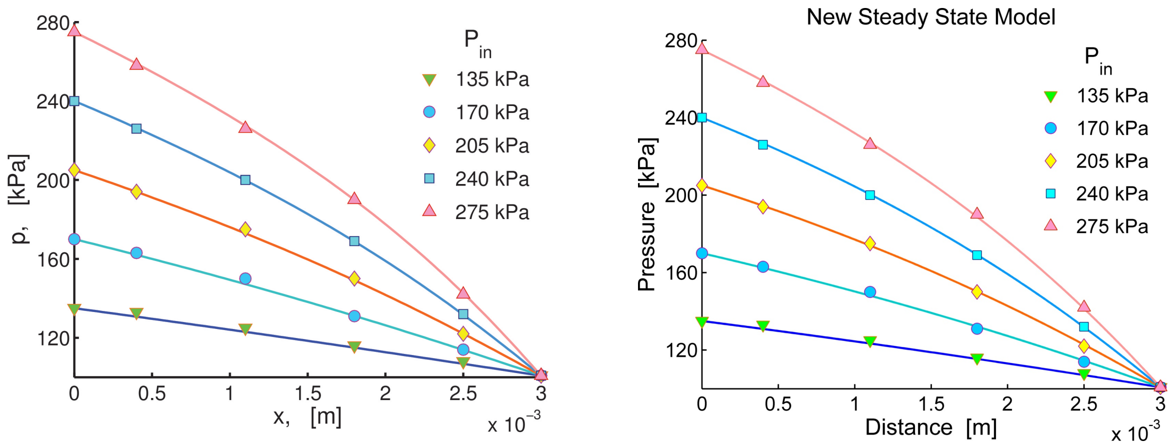

Figure 3: Pressure against distance along the core sample. Simulation (solid lines), and experimental data (symbols) from Pong et al (1994), for different inlet flow pressures P_{in}, as indicated. (a) Left: Steady state model with $F = 1$, and (b) Right: Steady state model with $F \neq 1$.

Pong's data-sets consist of measurements of pressure, p, along a shale rock core sample of lenght $L = 3mm$, at a number of stations, x, along the rock length; this is repeated for several different inlet pressures, $P_{in} = 135, 170, 205, 240, 257$ kPa. We solve the steady state transport model equation (5), adjusting the model parameters to match Pong et al's data, from which we estimate the rock properties.

To test the importance of retaining all model parameters to be pressure dependent throughout the simulations, sixteen different models are produced by taking each of the four basic compressibility coefficients $(\zeta_\rho, \zeta_K, \zeta_f, \zeta_\mu)$, independently, to be pressure-dependent or pressure-independent. The rock properties, K, and ϕ, are determined from the best fit model which yields the smallest error compared to the data. For more details see **?**.

4.2 Models without Forchhiemer's correction, $F = 1$

In the transport models in which non-linear corrections for high flow rates are not included, $F = 1$, there are thirteen model parameters. The simulation results, from Model 16 in Ali and Malik (2018) is shown as pressure against the distance x along the core sample in Fig 3(a). The simulation results (lines) are compared with the data Pong et al (1994) (symbols). All models match the data for the lowest inlet pressure $P_{in} = 135$ kPa, showing that these tests are insensitive to such types of models at low pressure pulses. But, most of the models are greatly in error of the data for the higher inlet pressures; Model 16 gives the smallest error among all models, about 1×10^{-4}. This illustartes to importance of pressure dependent parameters in as a modeling strategy in general.

However, the estimates of rock properties from Model 16 are, the porosity $\phi = 0.2$, and the rock permeability $K = 10^{-15}$ m^2, (or 10^6 nD). These values are close to previous models, but they are not typical of shale rocks.

4.3 Models witht Forchhiemer's correction, $F \neq 1$

We now include a non-zero turbulence correction factor, $F \neq 1$, to produce a new set of transport models. As the importance of retaining the pressure-dependence of all model parameters has already been established, here we consider only Model 16 with $F \neq 1$ as the base case – there are now four additional model parameters, a total of seventeen parameters. After some parameter adjustment, Fig. 3(b) shows the simulation results against the data. We observe an excellent match between the numerical solutions and the experimental data. The error between the simulated and the measured pressure values is about 6×10^{-5}, which is smaller than from Model 16 with $F = 1$, Fig. 3(a).

Importantly, the range of porosity is in the range $0.10 < \phi < 0.1038$, and the intrinsic permeability lies in the range $106 < K < 111$ nD. These are much more realistic of shale rocks than obtained from any previous model, we believe for the first time from such types of models.

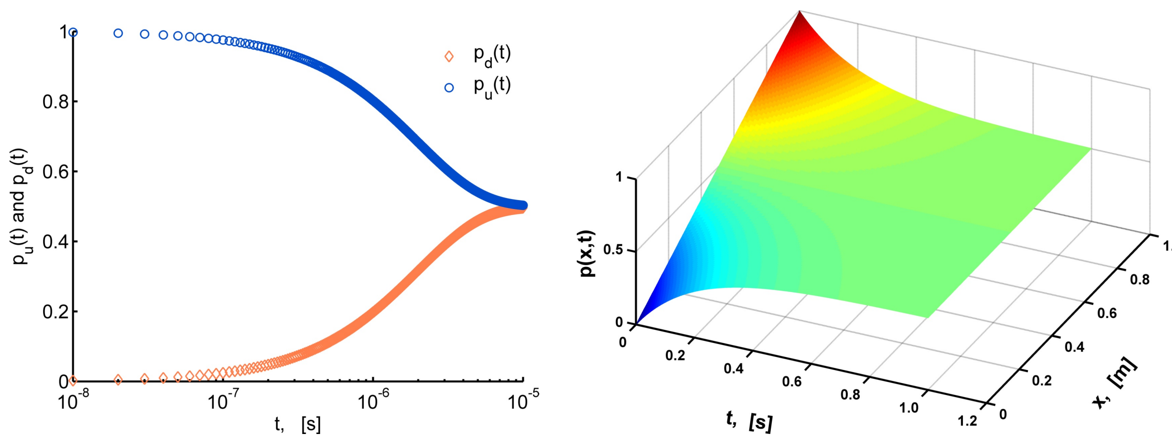

Figure 4: Pressure against distance along the core sample. Simulation (solid lines), and experimental data (symbols) from Pong et al (1994), for different inlet flow pressures P_{in}, as indicated. (a) Left: Steady state model with $F = 1$, and (b) Right: Steady state model with $F \neq 1$.

4.4 Forward Simulations: Transient Model

The transient transport model, equation (4), was used to simulate the pressure field in a shale rock core sample of length L over a period of time. Initial conditions are set as $p(x,0) = 0$ for $0 \leq x < 1$ and $p(x,0) = P$ for $x = 1$. Boundary conditions are set as $p(0,t) = p_d(t)$ for $t \geq 0$ and $p(L,t) = p_u(t)$ for $t \geq 0$. p_u is the pressure in the upstream reservoir, p_d is the pressure in the downstream reservoir.

We solve the transient nonlinear transport model (4) with initial and flux conditions to describe the pressure distribution in a rock core sample of length $L = 1$m to simulate pressure-pulse decay test. We obtain the pressure distribution under full pressure dependent reservoir parameters and compressibility coefficients. A pressure pulse is induced in the upstream reservoir at $t = 0$, which is attached to a core plug containing a rock sample. Figure 4 shows the results obtained from the numerical simulations.

5 Discussion and Conclusions

A fully pressure-dependent nonlinear transport model for the flow of shale gas in tight porous media developed in Ali and Malik (2018) was used to investigate rock properties and transient pressure fields. The transport model accounting for the important physical processes that exist in the system, such as continuous flow, transition flow, slip flow, surface diffusion, adsorption and desorption in to the rock material, and also including a nonlinear correction term for high flow rates (turbulence).

A steady state one-dimensional version of the model without gravity and without external source was used to determine shale rock properties by matching the pressure distribution across a shale rock core sample obtained from pressure-pulse decay tests for different inflow pressure conditions. The best estimates of rock properties was obtained when the high flow rate correction factor is included ($F \neq 1$) in the model, and when all model parameters are kept pressure dependent throughout the simulations, at high inlet pressure pulses. The estimates are much realistic than obtained from any previous transport models. The transient model was used for simulating future pressure field distribution inside a rock sample over a period of time.

We can draw the following conclusions. Firstly, a realistic transport model should incorporate all of the important physical transport sub-processes in the porous system. Secondly, model parameters and associated compressibility coefficients should be pressure dependent throughout the numerical procedure. Thirdly, a Forchchiemer correction term for high flow rates is essential for good estimation of rock properties. Pressure-pulse tests should be carried out at elevated pressure pulses.

Acknowledgements

The authors would like to acknowledge the support provided by King Abdulaziz City for Science and Technology (KACST) through the National Science, Technology and Innovation Plan (NSTIP), and through the

Science Technology Unit at King Fahd University of Petroleum & Minerals (KFUPM) for funding this work through project No. 14-OIL280-04.

References

Ali I., Chanane B., and Malik N.A. (2015) Compressibility coeffcients of nonlinear transport models in unconventional gas reservoirs. In: The 2015 AMMCS-CAIMS Congress, Springer, pp 1–10

Ali I. and Malik N.A. (2018) A realistic transport model with pressure dependent parameters for gas flow in tight porous media with application to determining shale rock properties. Transport In Porous Media, Vol. 123, No. 2, (2018). https://doi.org/10.1007/s11242-018-1092-4

Beskok A, Karniadakis GE (1999) Report: a model for flows in channels, pipes, and ducts at micro and nano scales. Microscale Thermophysical Engineering 3(1):43–77

Carman PC, Carman PC (1956) Flow of gases through porous media. Butterworths Scientific Publications London

Civan F (2010) Effective correlation of apparent gas permeability in tight porous media. Transport in porous media 82(2):375–384

Civan F, Rai CS, Sondergeld CH (2011) Shale-gas permeability and diffusivity inferred by improved formulation of relevant retention and transport mechanisms. Transport in Porous Media 86(3):925–944

Darishchev A, Rouvroy P, Lemouzy P (2013) On simulation of flow in tight and shale gas reservoirs. In: 2013 SPE Middle East Unconventional Gas Conference & Exhibition

Loeb LB (2004) The kinetic theory of gases. Courier Dover Publications

Liang Y, Price JD, Wark DA, Watson EB (2001) Nonlinear pressure diffusion in a porous medium: Approximate solutions with applications to permeability measurements using transient pulse decay method. Journal of Geophysical Research: Solid Earth (1978–2012) 106(B1):529–535

Malkovsky VI, Zharikov AV, Shmonov VM (2009) New methods for measuring the permeability of rock samples for a single-phase fluid. Izvestiya, Physics of the Solid Earth 45(2):89–100

Nia S, Dasani D, Tsotsis T, Jessen K (2013) Pore-scale characterization of oil-rich monterey shale: A preliminary study. In: Unconventional Resources Technology Conference

Pong K, Ho C, Liu J, Tai Y (1994) Non-linear pressure distribution in uniform microchannels. ASME-Publications-FED 197:51–51

Wang Y, Yan B, Killough J (2013) Compositional modeling of tight oil using dynamic nanopore properties. In: SPE Annual Technical Conference and Exhibition

Ziarani AS, Aguilera R (2012) Knudsen's permeability correction for tight porous media. Transport in porous media 91(1):239–260